

Differential responses to salt concentrations of lichen photobiont strains isolated from lichens occurring in different littoral zones

Francisco Gasulla¹, Alfredo Guéra¹, Asunción de los Ríos² & Sergio Pérez-Ortega^{3*}

Article info

Received: 27 May 2019
Revision received: 13 Sept. 2019
Accepted: 15 Sept. 2019
Published: 2 Dec. 2019

Associate Editor

Adam Flakus

Abstract. An interesting biota of lichen-forming fungi occurs along rocky seashores of cold and warm-temperate regions in both hemispheres. Most of the species belong to the family Verrucariaceae and form symbioses with an extraordinarily diverse group of photobionts. We isolated the photobionts of three species: *Hydropunctaria maura* and *H. amphibia* from the supralittoral zone, and *Wahlenbergiella striatula* from the upper intertidal zone. We characterized the isolated strains structurally by means of transmission electron microscopy, and molecularly using the nrSSU and nrITS and chloroplast RPL10A regions. Additionally, we studied the response of the strains to different salt concentrations, analyzed the concentration of osmoregulatory solutes, and measured photosynthesis performance by chlorophyll fluorescence and CO₂ assimilation techniques. All strains belong to the recently described species *Halofilum ramosum*, although we found differences in the ITS and RPL10A regions among the strains shared by *H. maura* and *H. amphibia* and the strain isolated from *W. striatula*. Differences were also found in the main osmoregulatory response of the strains growing under high salt concentrations: *W. striatula* accumulated glycerol, while *H. maura* and *H. amphibia* synthesized sucrose. Analyses of photosynthesis performance also indicated differences in physiological behavior between supralittoral-dwelling and intertidal-dwelling species, *W. striatula* showing lower photosynthetic activity under high irradiance. Our results highlight the role of photobionts in determining lichen zonation on rocky seashores.

Key words: *Halofilum*, *Hydropunctaria*, lichen-forming fungi, seashore, Verrucariaceae, *Wahlenbergiella*.

Introduction

Lichens, the symbiotic phenotype of a lichen-forming fungus (the mycobiont) and a eukaryotic alga and/or cyanobacterium (the photobiont), occur in most terrestrial habitats and cover ~8% of the land surface (Nash 2008). Lichens are able to thrive in the most extreme environments such as the hot and cold deserts of continental Antarctica, Chile (Atacama) and southwestern Africa (Namibia) (Green et al. 2012; Maphangwa et al. 2012). Rocky seashores are among the most extreme habitats, since organisms have to cope with highly influential abiotic factors such as fluctuating sun exposure, wave and wind action, daily cycles of desiccation and hydration,

contrasting temperature, and salinity levels (Knox 2000). Some lichens have adapted to live not only close to seawater but actually within the intertidal zone (Santesson 1939; Fletcher 1980; Taylor 1982; Brodo & Santesson 1997). On rocky seashores, species of lichen-forming fungi typically occur in more or less narrow bands which correspond to different intertidal zone immersion times or different levels of exposure to saline particles suspended in the air (spray) in the supralittoral zone (Fletcher 1973a, b). Furthermore, the species *Verrucaria serpuloides* from the Southern Hemisphere is known to grow permanently submerged (Lamb 1973).

The lichen biota occurring in the intertidal and supralittoral zones of temperate and cold oceans in both hemispheres is disharmonic as compared to the typical composition of lichen assemblages on rocks not affected by saltwater. Three lineages clearly dominate: (i) members of the order Collemopsidiales (Mohr et al. 2004; Pérez-Ortega et al. 2016), (ii) species of the genus *Lichina*

¹ Departamento de Ciencias de la Vida, Universidad de Alcalá, Campus Externo, 28805, Alcalá de Henares, Spain

² Museo Nacional de Ciencias Naturales (CSIC), Calle Serrano 115-dpdo, 28006, Madrid, Spain

³ Real Jardín Botánico (CSIC), Plaza Murillo 2, 28014 Madrid, Spain

* Corresponding author e-mail: s.perezortega@gmail.com

(Ortiz-Álvarez et al. 2015; Schultz 2017), and (iii) species from the family *Verrucariaceae* (Santesson 1939; Fletcher 1980; Taylor 1982; Brodo & Santesson 1997). Species of the recently described genus *Wahlenbergiella* occur in the intertidal zone of the Northern Hemisphere (Gueidan et al. 2009), whereas species of *Hydropunctaria* mostly occur in the supralittoral zone (Gueidan et al. 2009; Orange 2012).

Only a limited number of studies have attempted to elucidate the factors influencing the distribution of lichens on rocky seashores. Ortiz-Álvarez et al. (2015) showed that a particular strain of the cyanobacterial photobiont *Rivularia* was important in determining the distribution of two species of *Lichina* on rocky seashores of the Atlantic coast of Europe, suggesting that a photobiont switch was associated with speciation in this fungal lineage. Thus, physiological requirements of lichen photobionts could drive the distribution of mycobiont species at the seashore.

Marine species in the family *Verrucariaceae* show the most extraordinary range of compatible photobionts (Thüs et al. 2011), including associations with *Xanthophyceae* (Parra & Redon 1977; Thüs & Schultz 2008), *Phaeophyceae* (Moe 1997; Sanders et al. 2004), *Trebouxiophyceae* (Pérez-Ortega et al. 2010; Garrido-Benavent et al. 2017) and *Ulvophyceae* (Thüs et al. 2011; Darienko & Pröschold 2017; Pérez-Ortega et al. 2018). In contrast, there are no recorded associations between marine species and algal genera such as *Trebouxia*, *Asterochloris* or *Trentepohlia*, the most common taxa found in species from the order *Lecanorales*. Recent taxonomic work on the *Ulvophyceae* (Darienko & Pröschold 2017) has shown that filamentous photobionts previously ascribed to the genus *Dilabifilum* (e.g., Thüs et al. 2011) that were isolated from marine *Verrucariaceae* actually belong to the newly described lineage *Halofilum* and the genus *Pseudendoclonium*.

On rocky seashores, salinity is the main factor influencing lichen zonation (Delmail et al. 2013). At low shore levels, lichens are exposed to almost constant immersion in seawater, whereas at higher shore levels they are subjected to a changing osmotic environment that is hyperosmotic when wetted by surf and hypoosmotic during rainfall. The lower and upper shore limits of algae may depend largely on the adaptation of the species to preferred salinity levels and on tolerance to osmotic fluctuations. Furthermore, the presence of brackish water from the mixing of seawater with freshwater, as in river estuaries or tidewater glaciers, usually restricts the occurrence of most marine lichens. Microorganisms have developed several strategies to regulate their internal osmotic pressure to adjust to high or low external solute concentrations in order to avoid water loss and subsequently cell plasmolysis. One osmoadaptation strategy entails reliance on the efflux of inorganic ions from/to the surrounding environment (Pick 2002; Oren et al. 2008). The second strategy involves synthesis of low-molecular-weight organic compatible solutes to balance the external osmotic pressure. It has been observed that microalgae tend to accumulate three different kinds of osmoregulatory solutes, depending on their tolerance to salinity (Batterton & Baalen 1971; Stacey et al. 1977; Ben-Amotz & Avron 1981; Ben-Amotz & Grunwald 1981; Joset et al. 1996;

Page-Sharp et al. 1999): (i) low-halotolerant algae (less than 0.7 M NaCl) accumulate sugars such as sucrose or trehalose; (ii) medium-halotolerant algae (0.7–1.8 M NaCl) accumulate polyols like glucosylglycerol or mannitol; and (iii) high halotolerant alga (more than 1.8 M NaCl) accumulate amino acid compounds such as glycine, betaine or glutamate and glycerol.

The aim of this study was to determine the possible relation between the intertidal zonation of marine *Verrucariaceae* species, the halotolerance of their algal partners, and the physiological response to salt concentration. Photobionts of two species characteristically occurring in the supralittoral zone of the Iberian Peninsula's Atlantic coast (*Hydropunctaria maura* and *H. amphibia*) and one species occurring in the middle and lower parts of the intertidal zone (*Wahlenbergiella striatula*) were isolated and cultured under laboratory conditions. They were characterized by means of molecular and electron microscopy techniques, and their responses to decreasing salinity levels (from seawater to rainwater) were monitored using chlorophyll fluorescence, CO₂ assimilation, and concentration of osmoregulatory solutes.

Material and methods

Lichens studied; isolation and culture of their algal symbionts

Three species of marine *Verrucariaceae* typically occurring on rocky seashores along the north coast of the Iberian Peninsula were selected for this study. *Wahlenbergiella striatula* is characterized by a film-like, light to dark green thallus furrowed by numerous black ridges and perithecia (Fig. 1B). It occurs in the middle to upper intertidal zone and is known from Europe, North America, Australia and New Zealand (Santesson 1936; Orange 2013). The two other species, *Hydropunctaria amphibia* and *Hydropunctaria maura*, typically occur in the supralittoral zone. *Hydropunctaria amphibia*, distinguished by its black, more or less thick thallus, with characteristic carbonized linear structures reaching the thallus surface (Fig. 1C), occurs in the lower supralittoral zone, whereas *H. maura*, with a relatively thick thallus and small spots of carbonized tissue reaching the thallus surface (Fig. 1D), occurs in the upper supralittoral zone, although both species typically can be found growing side by side (Renobales & Noya 1991). All specimens were collected from rocky seashore at Playa del Silencio (Novellana, Asturias, 43°33'59"N; 6°35'62"W) by SPO and AdR (16 May 2010).

Isolation was done a few hours after sample collection. Small rock fragments including lichen thalli were rinsed in sterile water several times and surface-sterilized with alcohol. Afterwards, small fragments of the lichen thalli (~4 mm²) were removed with a scalpel blade, placed in a microcentrifuge tube with 200 ml of sterile water, then ground with a plastic micropestle. The mix was transferred to agar plates with artificial seawater medium (ASM) containing 30‰ (w/v) NaCl supplemented with vitamins (ASM30+V, modified from Starr & Zeikus 1993) and cultivated under constant temperature (22°C) and irradiance

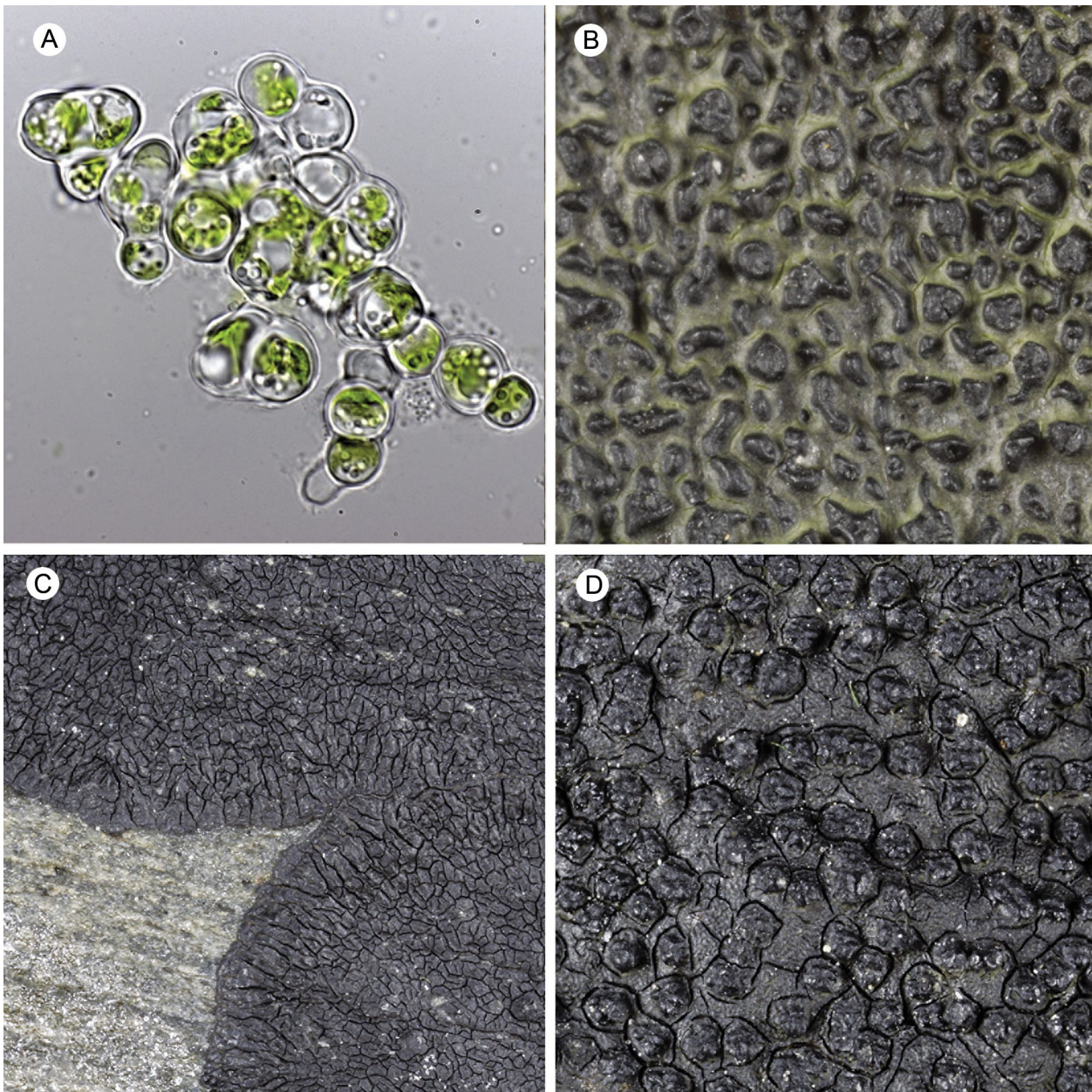


Figure 1. Habitus of isolated strains and lichens. A – *Halofilum ramosum* isolated from *Wahlenbergiella striatula* growing in artificial seawater medium containing 30‰ NaCl; B – *Wahlenbergiella striatula*; C – *Hydropunctaria amphibia*; D – *Hydropunctaria maura*. Scales: A = 10 μm ; B = 1 mm; C = 5 mm; D = 1 mm.

(PAR 84 mmol photons $\text{m}^{-2} \text{s}^{-1}$) provided by a combination of GroLux and cool-white fluorescent lamps. Single colonies were sampled after 45 days and transferred to 500 ml ASM30+V liquid medium. After 3 months, 100 ml aliquots were transferred to liquid growth media with contrasting salt (NaCl) concentrations: 30‰ (ASM30+V), 15‰ (ASM15+V) and 0‰ (ASM0+V). Cultures were kept under the same growth conditions for 3 months until they were used for analyses.

DNA extraction and phylogenetic analysis

DNA extraction was carried out using a Soil DNA Isolation Kit (MoBio Laboratories) according to the manufacturer's instructions and eluted in a final volume of 50 μL of H_2O . We amplified a fragment of the nrSSU region using the primer pair SR1 and SR7 (Nakayama et al. 1996), the nrITS region using the primer pair nr-SSU-1780

(Piercey-Normore and Depriest 2001) and ITS4 (White et al. 1990), and the hypervariable RPL10A region which encodes the RPL10 protein required for joining 40S and 60S subunits into a functional 80S ribosome (del Campo et al. 2013), using the primer pair Rf-RLaF and Rf-L10aR (del Campo et al. 2013). PCR reactions for the nrSSU region were performed in a total volume of 25 μL containing 3 μL of DNA template, 3 μL of 10 \times PCR buffer (Biotools), 6 μL of dNTPS, 0.9 μL of each primer, 0.9 μL of MgCl_2 , and 1.5 units of DNA polymerase (Biotools), adding distilled water to reach the final volume. PCR reactions for the nrITS and RPL10A regions were performed in a total volume of 25 μL containing Illustra™ PuReTaq RTG PCR Beads (GE Healthcare), 3 μL of DNA template, 1.25 μL of each primer, and 19.5 μL of H_2O . PCR amplifications were performed in a Biorad MJMini thermal cycler. The PCR conditions for the nrSSU region

were as follows: initial 4 min heating phase at 95°C, followed by 35 cycles of 1 min at 94°C, 1 min at 55°C and 2 min at 72°C, and a final extension step of 10 min at 72°C. PCR conditions for the nrITS region were as follows: initial 2 min heating phase at 94°C, followed by 35 cycles of 30 secs at 94°C, 30 secs at 56°C and 45 secs at 72°C, and a final extension step of 10 min at 72°C. The PCR conditions for the RPL10A region followed del Campo et al. (2013). The PCR products were purified using QIAquick PCR purification columns (Qiagen) according to the manufacturer's instructions and sequenced by Macrogen Inc. (Madrid, Spain) using the same primer sets as for PCR amplification. Sequence contigs were assembled using SeqMan v.14 (Lasergene, DNA Star Inc., WI, USA).

The sequences (nrSSU, nrITS) obtained in this study (Table 1) were aligned with members of *Ulvales* following the recent study by Darienko & Pröschold (2017). Alignments were carried out using MAFFT v.7.0 (Katoh et al. 2009) as implemented in Genious™ v.9.0.4 (Biomatters Ltd, New Zealand), using default parameters, and subsequently inspected by eye. Gblocks 0.91b (Castresana 2000) was used to remove ambiguously aligned regions and large gaps, using the least stringent parameters but allowing gaps in 50% of the sequences. Optimal nucleotide substitution models for the Bayesian analysis for each genomic region were established by means of jModelTest v.2 (Darriba et al. 2012) using the Akaike information criterion (nrITS: GTR+I+G; nrSSU: GTR+G). IQ-TREE (Nguyen et al. 2015; Kalyaanamoorthy et al. 2017) through its online version W-IQ-TREE (Trifinopoulos et al. 2016) implemented at <http://iqtree.cibiv.univie.ac.at>, was used for the heuristic search of the maximum likelihood (ML) tree and simultaneous inference of the substitution model for each data partition and the optimal partitioning scheme. Branch support was estimated with the ultrafast bootstrap algorithm (Minh et al. 2013). Bayesian inference of the phylogenetic relationships was carried out in MrBayes v.3.2 (Ronquist et al. 2012). Settings included two parallel runs with four chains over 10M generations, sampling every 1000th step. The first 25% of saved data was discarded as burn-in. Convergence of chains was confirmed by the convergent diagnostic of the potential scale reduction factor (PSRF), which approached 1, and inspected visually in Tracer v. 1.6 (<http://tree.bio.ed.ac.uk/software/tracer/>). Phylogenetic trees were visualized in FigTree v. 1.4.1 (<http://tree.bio.ed.ac.uk/software/figtree/>), and Adobe Illustrator CS2® was used for artwork. Strongly supported nodes were defined as those with ultrafast bootstrap values $\geq 90\%$ and Bayesian posterior probability ≥ 0.95 , shown in bold in Figure 2.

Analysis of osmoregulatory solutes

The concentrations of osmoregulatory solutes (glucose, glycerol, mannitol, sucrose, trehalose) in the algal strains isolated from the three lichens and growing in the three salt concentrations were assessed by means of high performance liquid chromatography (HPLC). Nine

samples of 1.4 ml were collected from cultures of each algal strain after one month growing in liquid media and centrifuged for 5 min at 10,000 g. Precipitated cells were frozen until use, when 50 mg of this frozen algal growth was resuspended in 1.5 ml of sterile distilled water and ground with a plastic micropestle. The mixture was subjected to ultrasonic baths for 3 min and later boiled for 5.5 min. Homogenates were centrifuged for 5 min at 10,000 g. Supernatants were decanted, filtered (nylon filter, 0.45 mm) and loaded (50 ml) on a cationic exchange column (Hamilton RCX-10, 4.6 mm \times 25 cm) maintained at room temperature. A 0.2% sodium hydroxide solution was used as mobile phase (2 ml/min). Detection was performed with a pulsed amperometric detector.

Ultrastructural characterization of algal strains

Samples for study of algal strain ultrastructure were prepared following de los Ríos & Ascaso (2002). In brief, algal cells were fixed in glutaraldehyde, postfixed in osmium tetroxide and then dehydrated in a graded series of ethanol before embedding in Spurr's resin. Semi-thin (0.35 mm) and ultrathin (70 nm) sections were prepared with a diamond knife, using a Reichert Ultracut-E ultramicrotome, and post-stained with lead citrate (Reynolds 1963). Sections were observed with a Zeiss EM910 transmission electron microscope.

Photosynthesis and chlorophyll fluorescence measurements

Photobiont cells from all algal strains and salt concentrations were harvested (~200 mg) with nylon filters (5 μ m pore-size), transferred to solid media and maintained under the same culturing conditions for 24 h. The response of photobiont net assimilation rate (A) to changing external photosynthetically active radiation (PAR) was measured using a LCpro + Portable Photosynthesis System (ADC Bioscientific Ltd., Hertfordshire, UK). Rates of CO₂ uptake were related to weight. The response of A to changing PAR was assessed following 5 min stepwise increases in PAR from darkness to 1000 μ mol photons m⁻² s⁻¹ at a CO₂ concentration of 400 ppm at 20°C.

Chlorophyll *a* fluorescence was measured at room temperature using a pulse modulation fluorometer (PAM-2000, Walz, Effeltrich, Germany). Algae samples were layered on filter paper that was kept moist with distilled water in order to maintain the cells in a fully hydrated state. The samples were kept in the dark for 30 min, after which the minimal fluorescence yield (F_o) was obtained by exciting the photobionts with a weak measuring beam from a light-emitting diode. The maximum fluorescence yield (F_m) was determined with an 800 ms saturating pulse of white light (8000 μ mol m⁻² s⁻¹ PAR). Variable fluorescence in dark-adapted samples (F_v) was calculated as F_m-F_o. The maximum quantum yield of photosystem II (PSII) was calculated as F_v/F_m (Kitajima and Butler 1975). Next, a 90 s stepwise increase in PAR followed by saturating pulses of white light were applied to determine (i) maximum fluorescence yield during actinic illumination (F_m'), (ii) Chl *a* fluorescence yield during actinic

Table 1. GenBank accession numbers and collection information for the strains included in the phylogenetic analyses. New sequences are bolded.

Strain No.	Taxonomy	Origin	nrSSU Accession N°	nrITS Accession N°	RPL10A Accession N°
CCMP 2158	<i>Ctenocladius circinnatus</i> 1	Italy, Pompei, from ruins	MF034603	MF034603	–
ULYO-16	<i>Ctenocladius circinnatus</i> 3	Ukraine, Kherson Oblast, Azov-Syvash National Park, solonchak (hyperhaline soil)	MF034604	MF034604	–
ULYO-17	<i>Ctenocladius circinnatus</i> 4	Ukraine, Kherson Oblast, Azov-Syvash National Park, solonchak (hyperhaline soil)	MF034605	MF034605	–
ULYO-18	<i>Ctenocladius circinnatus</i> 2	Luxembourg, Casemate 'Petruș', Fort Bourbon	MF034606	MF034606	–
ULYO-24	<i>Ctenocladius circinnatus</i> 5	Ukraine, Odesa Oblast, Snake Island, quartz, epilithic	MF034607	MF034607	–
ULYO-25	<i>Ctenocladius circinnatus</i> 6	Ukraine, Odesa Oblast, Kuyalnyk, solod (hyperhaline soil)	MF034608	MF034608	–
SAG 467-2	<i>Pseudodoclonium arthopyreniae</i>	Germany, Wangerooge, photobiont of lichen <i>Arthopyrenia kelpii</i> on snail shell of <i>Littorina littorea</i>	MF034609	MF034609	–
CCAP 415/1	<i>Pseudodoclonium incrustans</i>	Austria, photobiont of lichen <i>Verrucaria aquatilis</i>	MF034610	MF034610	–
SAG 23-92	<i>Paulbroadya prostrata</i> 1	Antarctica, Ross Island, Cape Royds, green epilithic crusts on rocks	MF034611	MF034611	–
CCAP 415/4	<i>Paulbroadya prostrata</i> 2	Antarctica, Ross Island, Cape Royds, green epilithic crusts on rocks	MF034612	MF034612	–
SAG 467-1	<i>Ctenocladius printzii</i>	Switzerland, Rosenau/Basel, bog water	MF034613	MF034613	–
SAG 2038	<i>Lithotrichum pulchrum</i>	Germany, Gladenbacher Bergland, near Dillenburg and Wetzlar, submers from lichen <i>Verrucaria rheitrophila</i>	MF034614	MF034614	–
SAG 2050	<i>Halofilum ramosum</i> 2	United Kingdom, Wales, Anglesey, Porth Treceastel, in stonerecks of coastal rocks, isolated from lichen <i>Wahlenbergiella striatula</i>	MF034615	MF034615	–
SAG 2051	<i>Pseudodoclonium commune</i> 1	United Kingdom, Wales, Anglesey, Aberffraw, on coastal rocks (Pelvetia-zone)	MF034616	MF034616	–
SAG 2235	<i>Halofilum ramosum</i> 3	France, North Atlantic, Roscoff, Brittany, photobiont of <i>Verrucaria maura</i>	MF034617	MF034617	–
SAG 2236	<i>Pseudodoclonium commune</i> 2	France, North Atlantic, Öland, photobiont of <i>Verrucaria maura</i>	MF034618	MF034618	–
SAG 2237	<i>Pseudodoclonium submarinum</i> 1	Scotland, North Atlantic, Oban, photobiont of <i>Verrucaria mucosa</i>	MF034619	MF034619	–
SAG 2240	<i>Paulbroadya petersii</i> 1	France, North Atlantic, Roscoff, Brittany, photobiont of <i>Verrucaria mucosa</i>	MF034620	MF034620	–
ULYO-19	<i>Halofilum ramosum</i> 1	Tunisia, Carthage, archeological remains, green biofilm on wall	MF034621	MF034621	–
ULYO-21	<i>Pseudodoclonium commune</i> 3	Ukraine, Odesa Oblast, Snake quartz, epilithic	MF034622	MF034622	–
ULYO-26	<i>Pseudodoclonium submarinum</i> 2	France, North Atlantic, Roscoff, Brittany, photobiont of <i>Verrucaria maura</i>	MF034623	MF034623	–
ULYO-28	<i>Halofilum ramosum</i> 4	France, North Atlantic, Roscoff, Brittany, photobiont of <i>Verrucaria maura</i>	MF034624	MF034624	–
ULYO-34	<i>Paulbroadya petersii</i> 2	Scotland, North Atlantic, Oban, photobiont of <i>Verrucaria mucosa</i>	MF034625	MF034625	–
SAG 1.95	<i>Halofilum salinum</i>	France, Schorre de estuary of the river Orne at Sallenelles, from a piece of wood	MF034634	MF034634	–
SAG 2.95	<i>Halofilum helgolandicum</i>	Germany, Schleswig-Holstein, Helgoland, from an enrichment culture of <i>Rhizoclonium riparium</i>	MF034635	MF034635	–
CCAP 6006/1	<i>Desmochloris halophila</i>	South Africa, Flaminckvlakte, the western Succulent Karoo, in soil crusts	FM882216	FM882216	–
CCAP 6006/2	<i>Desmochloris mollenhaueri</i> 1	South Africa, Flaminckvlakte, the western Succulent Karoo, in soil crusts	FM882217	FM882217	–
CCAP 6006/3	<i>Desmochloris mollenhaueri</i> 2	South Africa, Flaminckvlakte, the western Succulent Karoo, in soil crusts	FM882217	FM882217	–
Hr-Ha	<i>Halofilum ramosum</i> Ha	Spain, Novellana, Playa del Silencio, isolated from <i>Hydropunctaria amphibia</i> MA-Lichen 20537	MN545616	MN545616	MN551199
Hr-Ws	<i>Halofilum ramosum</i> Ws	Spain, Novellana, Playa del Silencio, isolated from <i>Wahlenbergiella striatula</i> MA-Lichen 20538	MN545615	MN545615	MN551198
Hr-Hm	<i>Halofilum ramosum</i> Hm	Spain, Novellana, Playa del Silencio, isolated from <i>Hydropunctaria maura</i> MA-Lichen 20536	MN545614	MN545614	MN551197

illumination (F_s), and (iii) the level of modulated fluorescence during brief interruption (3 s) of actinic illumination in the presence of $6 \mu\text{mol photons m}^{-2} \text{s}^{-1}$ far-red light (F_o'). The non-photochemical dissipation of absorbed light energy (NPQ) was determined at each saturating pulse according to the equation $\text{NPQ} = (F_m - F_m')/F_m'$ (Bilger and Björkman 1991). The quantum efficiency of PSII photochemistry (Φ_{PSII}), closely associated with the quantum yield of non-cyclic electron transport, was estimated from $(F_m' - F_s)/F_m'$ (Genty et al. 1989). The relative electron transport rate (ETR) was calculated as $\Phi_{\text{PSII}} \times \text{PAR} \times 0.84 \times 0.5$ (Schreiber et al. 1986). Excitation pressure on PSII, which reflects the proportion of the primary quinone electron acceptor of PSII that is in the reduced state, was calculated as $1 - qP$ (Demmig-Adams et al. 1990), where qP is the coefficient of photochemical quenching (van Kooten & Snel 1990).

Results

Molecular characterization of algal strains

Bayesian and maximum likelihood analyses of the nrSSU-ITS dataset produced similar topologies, and only the Bayesian 50% majority-rule consensus tree is depicted

in Figure 2. Recovered phylogenetic relationships among genera in Ulvales mostly agreed with the topology obtained by Darienko & Pröschold (2017). The only difference was that we recovered *Desmochloris* in a well-supported position as basal to the clade made up of *Lithotrichon*, *Pseudendoclonium*, *Paulbroadya* and *Halofilum*, whereas Darienko and Pröschold (2017) recovered the latter clade as sister to *Ctenocladus* but not statistically supported. The strains isolated from *Hydropunctaria amphibia* (hereafter Hr-Ha), *H. maura* (hereafter Hr-Hm) and *Wahlenbergiella striatula* (hereafter Hr-Ws) clearly belong to the species *Halofilum ramosum* (Fig. 2).

All nrSSU sequences obtained from the isolated strains were identical to available sequences of *Halofilum ramosum*. The nrITS sequences from Hr-Ha and Hr-Hm were identical and differed in four positions from the most similar *H. ramosum* strains: SAG 2235 (MF034617) and ULVO-28 (MF034624), both isolated from *H. maura* from northern France. On the other hand, strain Hr-Ws differed in two positions and a 3 bp deletion from strains Hr-Ha and Hr-Hm. The sequence of the hypervariable region RPL10A from Hr-Ws differed in 13 (2.53%) of 513 positions from the sequences of Hr-Ha and Hr-Hm, which were identical in those two strains.

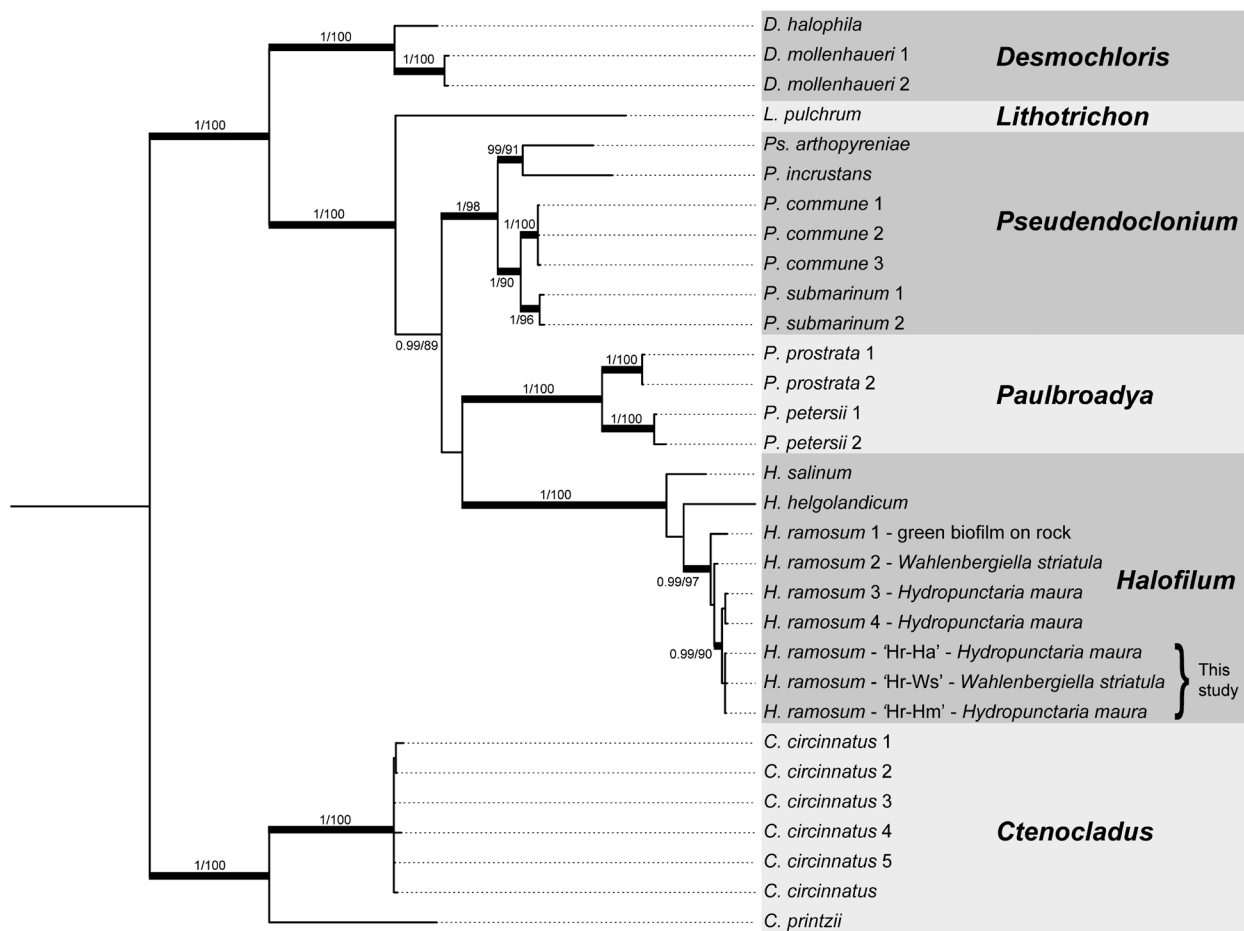


Figure 2. Bayesian 50% majority-rule consensus tree based on the combined nrSSU and nrITS regions, showing phylogenetic relationships among genera in the Ulvales and the phylogenetic affinity of the isolated strains in this study with *Halofilum ramosum*. Posterior probability and ultrafast bootstrap values are indicated close to the nodes. Branches in boldface represent nodes supported by both analyses. For *Halofilum ramosum*, the source from which the strains were isolated is given after the dash.

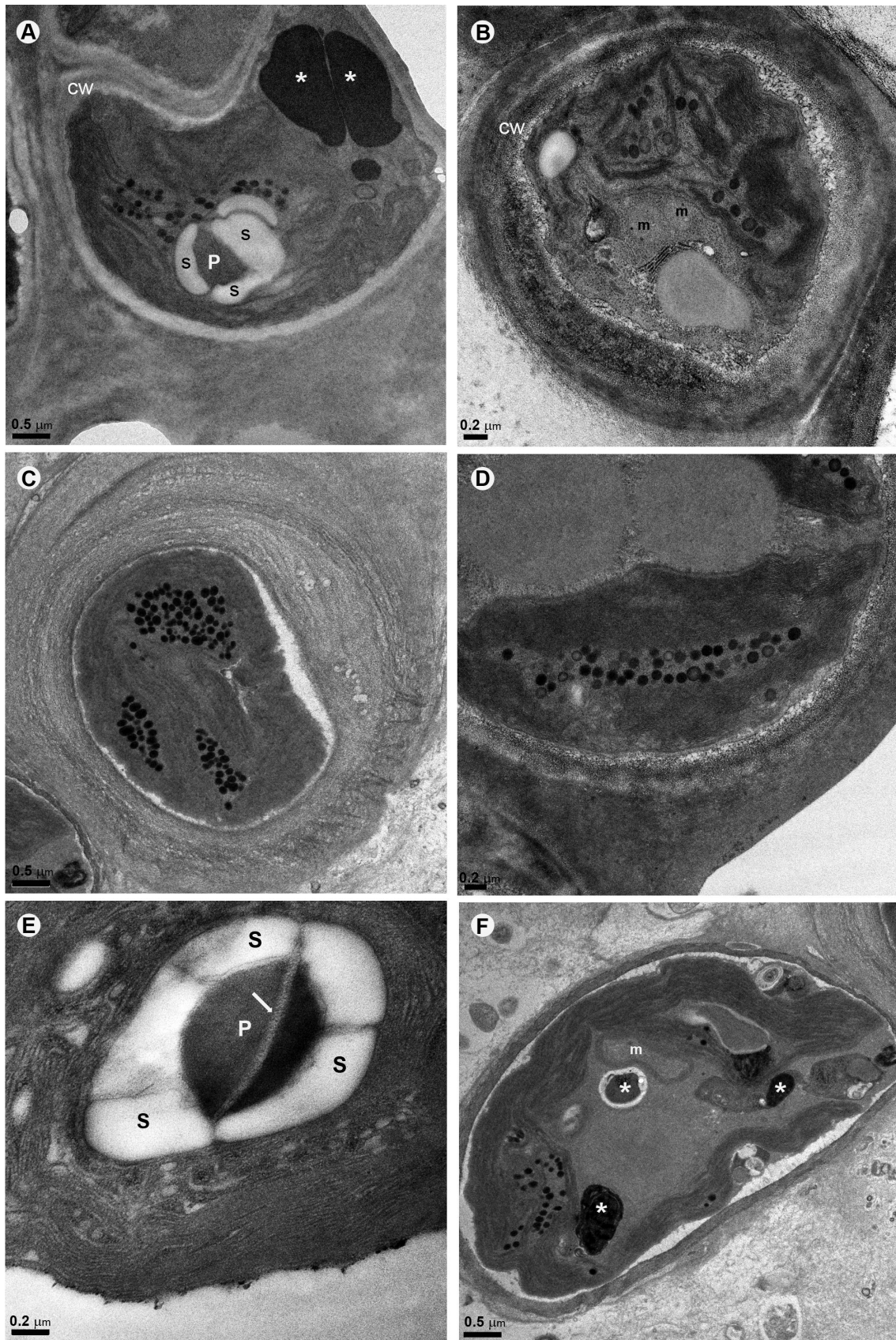


Figure 3. TEM images of cultivated photobionts from *Wahlenbergiella striatula*, *Hydropunctaria amphibia* and *Hydropunctaria maura* thalli. A – Photobiont cell from *W. striatula*, showing parietal chloroplast with pyrenoid (P) surrounded by starch plates (S) and multilayered cell wall (cw) and cytoplasmic osmiophilic structures (asterisks); B – Photobiont cell from *H. maura*, showing a parietal chloroplast with plastoglobuli situated between lamelas and several mitochondria (m) and multilayered cell wall (cw); C – Photobiont cell from *H. amphibia*, showing the majority of the cell volume occupied by the chloroplast and numerous plastoglobuli; D – Chloroplast of *H. maura* photobiont cell, showing a group of plastoglobuli in the central area of the chloroplast; E – Pyrenoid (P) of *W. striatula* photobiont cell surrounded entirely by starch grains (S) and penetrated by tubules (arrow); F – *H. amphibia* photobiont cell, showing parietal chloroplast and cytoplasm containing different osmiophilic structures (asterisks).

Ultrastructure of algal strains

The three isolates were morphologically similar and corresponded to uniseriate filaments of more or less roundish cells (Hr-Ws shown in Fig. 1D), although in some cultures elongated cells were also found. They had uninucleate cells and a single parietal chloroplast (Fig. 3A, B). In all of them, the chloroplast occupied much of the algal cell volume and plastoglobuli occurred between lamellas (Fig. 3A–D). In chloroplasts of Hr-Ws cells there was a conspicuous pyrenoid surrounded almost entirely by starch and penetrated by transpyrenoidal membranes (tubules) (Fig. 3A, E). Plastoglobuli were absent from this pyrenoid, and the surrounding starch plates appeared slightly spaced. The presence of numerous osmiophilic globules (Fig. 3A, B, F) and mitochondria (Fig. 3B) was frequent in several cells analysed in all cultures. The cell walls showed a similar distinct layered structure in all three isolates (Fig. 3B, D, F).

Carbohydrate quantification

HPLC analysis showed that *H. ramosum* strains accumulate glycerol and sucrose in high amounts ($2\text{--}24\text{ mg}\cdot\text{g}^{-1}$ DW). The presence of other carbohydrates such as mannitol, glucose and trehalose was also detected but in much

lower concentrations ($<1\text{ mg}\cdot\text{g}^{-1}$ DW) (data not shown) and was not analysed further. In Hr-Hm and Hr-Ha the amount of sucrose increased with salt concentration. In Hr-Hm, sucrose increased from $\sim 4\text{ mg}\cdot\text{g}^{-1}$ DW in 0‰ medium to $10.4\text{ mg}\cdot\text{g}^{-1}$ DW in 30‰ medium. In Hr-Ha, sucrose increased from $\sim 4\text{ mg}\cdot\text{g}^{-1}$ DW in 0‰ medium to $6.8\text{ mg}\cdot\text{g}^{-1}$ DW in 30‰ medium. In Hr-Ws, sucrose decreased from 9.8 to $2.6\text{ mg}\cdot\text{g}^{-1}$ DW under the same conditions (Fig. 4A). The response of glycerol displayed the opposite behaviour: in Hr-Ws the highest concentrations were found in algae growing in 30‰ medium, while in Hr-Hm and Hr-Ha the lowest concentrations were found in 0‰ medium (Figure 4B).

Photosynthesis performance

According to F_v/F_m measurements (Fig. 5), photosynthesis in the *Halofilum ramosum* strains seemed not to be affected by growth at different salt concentrations. Hr-Hm showed a gradual increase of F_v/F_m with salt concentration, but the difference between the highest value (0.633) at 30‰ NaCl and the lowest value (0.572) at 0‰ NaCl was less than 10%. For Hr-Ha there was no clear pattern of NaCl effect on F_v/F_m ; the F_v/F_m value was highest at 15‰ (0.689) and lowest at 30‰ (0.609). In Hr-Ws, F_v/F_m varied between 0.665 at 0‰ and 0.588 at 15‰.

The relative electron transport rate (ETR) was saturated at $800\text{--}1000\text{ }\mu\text{mol photons m}^{-2}\text{ s}^{-1}$ (PPDF) in all *H. ramosum* strains. The maximum values of ETR in Hr-Hm (Figure 6A) and Hr-Ha (Figure 6B) were higher (50–60) than in Hr-Ws (~ 40 , Figure 6C). As with F_v/F_m , the salinity of the medium did not have significant effects on ETR. Only in the case of Hr-Hm was the electron transport rate slightly lower when it grew in 0‰ NaCl medium. In Hr-Hm and Hr-Ha the increase of NPQ at higher light intensity was small, and was similar for algae grown under the different NaCl concentrations. However, in Hr-Ws the NPQ value increased steeply at higher light intensities, especially for algae grown at 0‰ NaCl (Fig. 6F).

Photosystem II (PSII) excitation pressure, expressed as $1\text{--}qP$ (photochemical quenching), increased gradually with light intensity in the three strains, showing similar

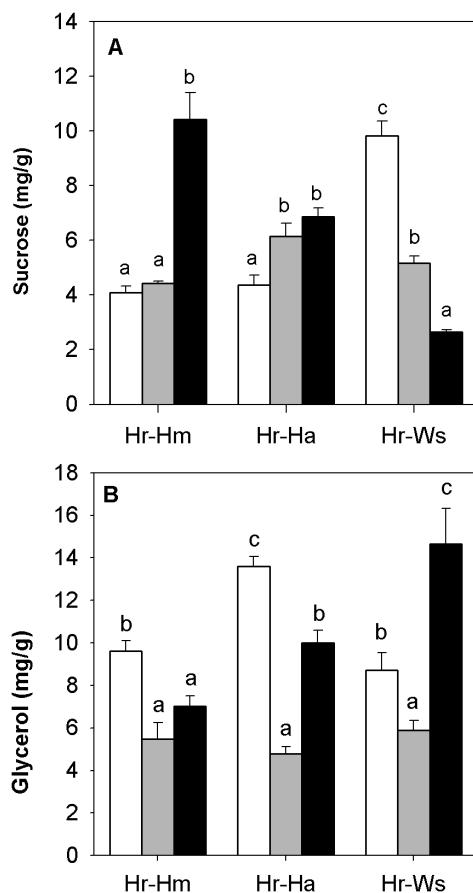


Figure 4. The concentration of sucrose (A) and glycerol (B) was quantified by HPLC in the different *Halofilum ramosum* (Hr) strains from the lichens *Hydropunctaria maura* (Hr-Hm), *H. amphibia* (Hr-Ha) and *Wahlenbergiella striatula* (Hr-Ws) growing in artificial seawater medium containing 0 (white), 15 (grey) or 30‰ (black) NaCl. Bars represent means \pm SE, $n = 9$. Values bearing different letters differ significantly ($p < 0.05$) by Fisher test (LSD).

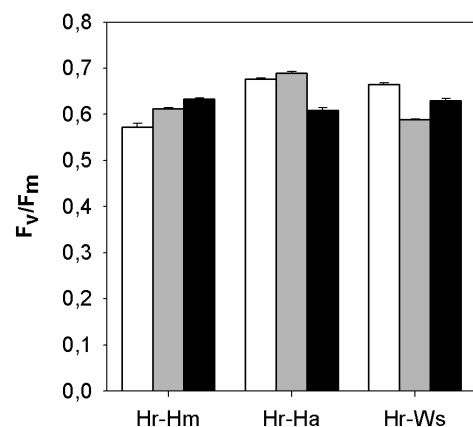


Figure 5. Maximum fluorescence yield (F_v/F_m) of the different *Halofilum ramosum* strains (Hr), ecotypes from the lichens *Hydropunctaria maura* (Hr-Hm), *H. amphibia* (Hr-Ha) and *Wahlenbergiella striatula* (Hr-Ws) growing in artificial seawater medium containing 0 (white), 15 (grey) or 30‰ (black) NaCl. Bars represent means \pm SE, $n = 4\text{--}5$.

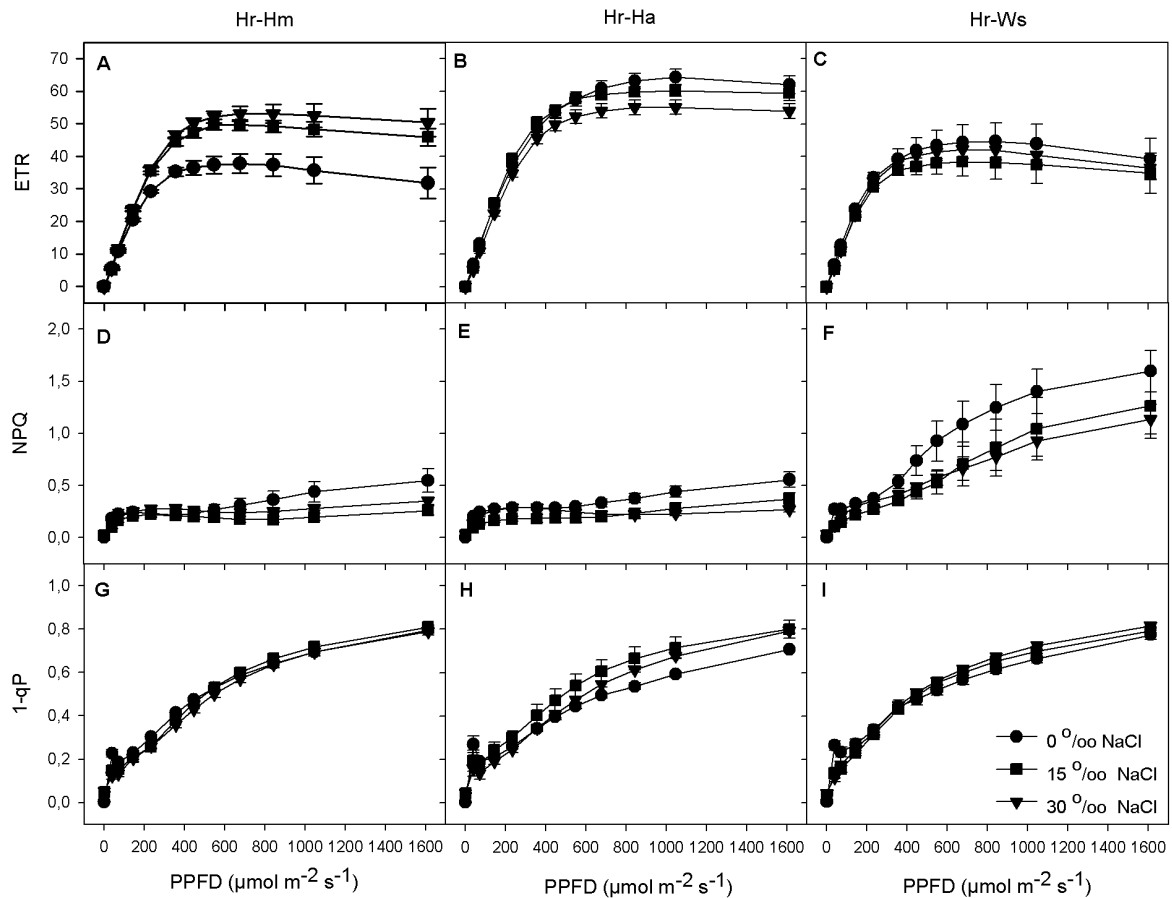


Figure 6. PPFD response curves of the relative electron transport rate (ETR) (A, B, C), non-photochemical quenching (NPQ) (D, E, F) and PSII photooxidative pressure (1-qP) (G, H, I) in the different *Halofilum ramosum* (Hr) strains from the lichens *Hydropunctaria maura* (Hr-Hm) (A, D, G), *H. amphibia* (Hr-Ha) (B, E, H) and *Wahlenbergiella striatula* (Hr-Ws) (C, F, I) growing in artificial seawater medium containing 0, 15 or 30‰ NaCl. Bars represent means \pm SE, $n = 4-5$.

values for all samples independently of NaCl content in the growth media (Fig. 6G–I).

CO₂ assimilation light saturation curves (Fig. 7) showed a low light compensation point ($\sim 0 \mu\text{mol CO}_2 \text{ m}^{-2} \text{ s}^{-1}$) for all cases studied. The CO₂ assimilation light saturation point was greater for all strains grown without NaCl. In addition, the measurements of CO₂ gas exchange showed that Hr-Hm and Hr-Ha had the highest assimilation rates, reaching values of $\sim 1 \mu\text{mol CO}_2 \text{ m}^{-2} \text{ s}^{-1}$ at 600–800 PPFD (Fig. 7A, B), while in Hr-Wm the assimilation of CO₂ in Hr-Wm was $\sim 50\%$ lower (Fig. 7C).

Discussion

All seashore-dwelling lichens from the northern coast of the Iberian Peninsula studied here had *Halofilum ramosum* as photobiont. Previous studies (e.g., Thüs et al. 2011) indicated that most marine Verrucariaceae had members of the genus *Dilabifilum* as photobionts. Darienko & Pröschold (2017) recently reviewed the taxonomy of aquatic members of the order *Ulvales* and showed that *Dilabifilum* is a later synonym of *Pseudendoclonium*. At least two species of this genus, *P. arthopyreniae* and *P. commune*, are known to be present in lichen symbioses, the latter isolated from *Hydropunctaria maura* from Sweden (Darienko & Pröschold 2017). Those authors

also described *Halofilum*, a genus characterized by short-branched and easily disintegrating filaments, vegetative cells with a parietal chloroplast containing a pyrenoid, and reproduction occurring by budding or vegetative division (Darienko & Pröschold 2017). Our cultures isolated from *Wahlenbergiella striatula*, *Hydropunctaria maura* and *H. amphibia* fit well with the molecular concept of *H. ramosum*. The isolated strains, however, differ morphologically from the strain shown in Darienko and Pröschold (2017). Although our strains form clear filaments, the cells are usually not elongated but irregularly rounded. Differences could come from the use of different culture media or from strains at different physiological states. Future studies should compare the morphology of identical strains growing on different culture media.

We found two strains differentiated at the molecular level at the variable nrITS region and the hypervariable RPL10A region, although not at the nrSSU region. Photobiont strains isolated from supralittoral species (*Hydropunctaria* spp.) shared the same photobiont strain (with identical nrSSU, nrITS and RPL10A sequences), whereas *Wahlenbergiella striatula*, a species growing in the upper intertidal zone, had a different strain. The ultrastructure of the cells from the three isolates also differed; only *W. striatula* photobiont cells showed a conspicuous pyrenoid surrounded by starch plates. A similar pyrenoid was

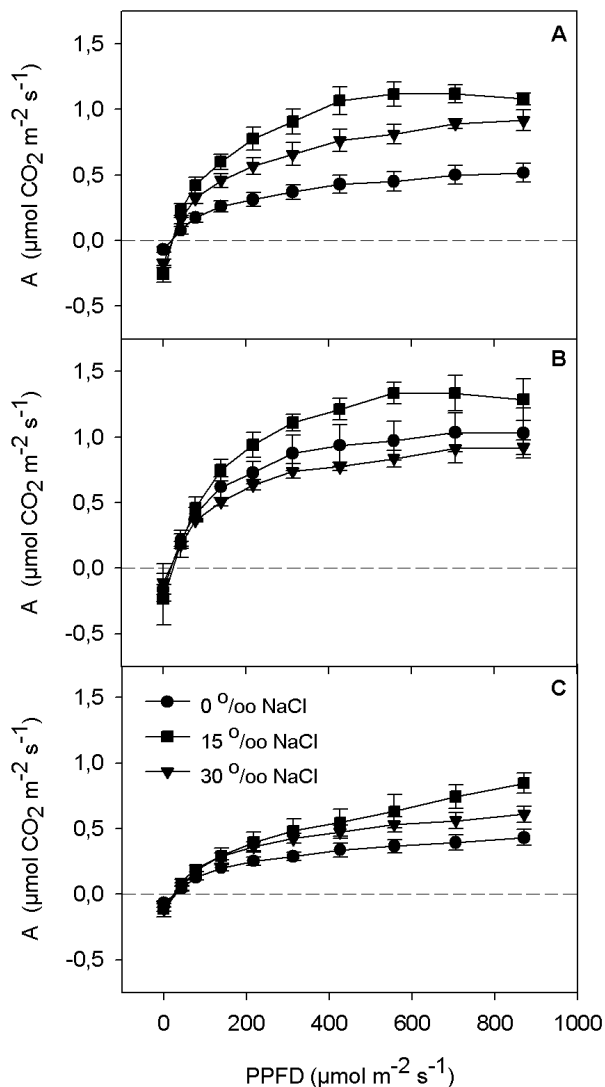


Figure 7. PPFD response curves of the net CO₂ assimilation rate in the different *Halofilum ramosum* strains from the lichens *Hydropunctaria maura* (A), *H. amphibia* (B) and *Wahlenbergiella striatula* (C) growing in artificial seawater medium containing 0, 15 or 30‰ NaCl. Bars represent means \pm SE, n = 4–5.

previously inferred for *H. ramosum* by means of light microscopy (Darienکو & Pröschold 2017). The presence of this type of pyrenoid could facilitate photosynthetic CO₂-fixing activity when *W. striatula* is submerged and low-CO₂ conditions prevail (Ramazanov et al. 1994; Zhan et al. 2018). In fact, the pyrenoid is considered to be a plastic organelle which can change in morphology, structure and composition in response to endogenous and external factors (Meyer et al. 2017). These molecular and ultrastructural differences, together with the different ecophysiology (see below), raise questions about the biological meaning of these divergences and about whether they indicate ecotypes or different species. Ortiz-Álvarez et al. (2015) studied the photobionts associated with two sister species of the lichen-forming fungi of the genus *Lichina* occurring in the intertidal zone (*L. pygmaea*) and the supralittoral zone (*L. confinis*). They found that the cyanobacteria associated with each species had diverged at \sim 170 mya, much earlier than the origin of the genus *Lichina*, suggesting an ecological speciation event

mediated by a photobiont switch that allowed invasion of a new ecological niche (Ortiz-Álvarez et al. 2015). Further research is needed to determine whether similar switches occurred in marine Verrucariaceae, but evidence points towards a much more complex scenario, with several lineages of associated photobionts (Moe 1997; Pérez-Ortega et al. 2010; Thüs et al. 2011; Pérez-Ortega et al. 2018) and Verrucariaceae lineages (Gueidan et al. 2007; Pérez-Ortega et al. 2018).

Algae have developed several biochemical strategies to maintain cell homeostasis under hyperosmotic stress; these include the capacity to synthesize and to accumulate compatible organic osmolytes. The presence of different low molecular weight carbohydrates such as arabinol, ribitol, mannitol, sorbitol, glycerol, sucrose, glucose and trehalose has been reported in lichens and their photobionts (Hill & Ahmadjian 1972; Roser et al. 1992; Armstrong & Smith 1994). HPLC analysis showed that glycerol and sucrose were the main osmolytes in all the *H. ramosum* ecotypes; however, their response to salinity was different in each strain. While sucrose was accumulated in Hr-Hm and Hr-Ha growing under high salinity, glycerol was synthesized in Hr-Ws. Several studies have demonstrated that the degree of halotolerance in algae is directly linked to the type of osmolyte that accumulates (Bremauntz et al. 2011, and references within). In stenohaline algae, sucrose is more often accumulated in response to osmotic stress, while in euryhaline species, glycerol is more commonly synthesized to adapt to high external salinity (Reed et al. 1984; Warr et al. 1985; Reed 1989). It is not clear what the advantage is for euryhaline algae to accumulate glycerol instead of sucrose. One possibility involves the difference in the energetic cost of accumulation of each osmolyte. Synthesis of the C12 disaccharide sucrose requires 109 ATP equivalents, while the C3 molecule glycerol demands only 30 ATP equivalents for its biosynthesis (Erdmann & Hagemann 2007). Another possibility is that osmolytes have to allow optimum enzymatic activity at high solute concentrations. It has been observed that high concentrations of sucrose can inhibit certain enzymes (Hinton et al. 1969). On the other hand, high concentrations of glycerol (>4 M) allow normal activity of intracellular enzymes in the euryhaline green algal genus *Dunaliella* (*Volvocales*) (Cowan et al. 1992; Bisson & Kirst 1995). This may explain why glycerol is the main osmolyte in algae growing at high salinity, sometimes approaching saturation (Hellebust 1985). The carbon source for synthesis of glycerol is via starch degradation (Hellebust 1985). In the euryhaline algae *Dunaliella tertiolecta*, the contribution of starch breakdown products to glycerol synthesis increased progressively with increasing salt stress (Goyal 2007). Interestingly, only Hr-Ws accumulated starch in the plastids, which might be employed for synthesis of glycerol. Thus, the analysis of organic osmolytes indicates that Hr-Ws might behave as an euryhaline alga, whereas Hr-Ha and Hr-Hm might be steno- or mesohaline species. It has to be noted, though, that the osmolytes produced in culture might be different from those produced by the same algae in symbioses. Future studies should address this question.

The maximum quantum yield of primary photochemistry in dark-adapted leaves (F_v/F_m) is the most common parameter used to express the physiological fitness of a plant, as assessed by fluorescence. Healthy plants reach F_v/F_m values around 0.840, but for lichens this parameter ranges between 0.550 and 0.700. The decline in the value of this parameter is generally attributed to photoinhibition of PSII associated with damage of the reaction centers. We found only small differences of F_v/F_m among the different strains and the different treatments. In addition, there were no clear trends in the variation of F_v/F_m in relation to NaCl concentration. Thus, our results indicate that *H. ramosum*, known so far only from marine environments (Darienko & Pröschold 2017), could be able to grow both in freshwater and in seawater. Seepage of freshwater from sea glaciers and river mouths decreases the salt concentration, influencing the distribution of lichens (Ryan 1988). The ability to cope with brackish waters represents a clear advantage for these *Halofilum* strains. Further studies should focus on determining the tolerance of the three phycobionts to higher salinity.

Fluctuation of solar radiation is another important environmental factor that may affect the distribution of marine lichens within the littoral zone (Ryan 1988), since the duration and intensity of irradiation will depend on the flooding altitude. We generated PPF curves to determine the response of photosynthesis to light intensity. The relative electron transport rate (ETR) was higher in Hr-Hm and Hr-Ha than in Hr-Ws, and the measurements of CO₂ gas exchange showed that Hr-Hm and Hr-Ha also had higher assimilation rates. Higgins et al. (2014) observed that photosynthetic yield in *Wahlenbergiella mucosa* was in general lower than in *Hydropunctaria maura*. Both *W. mucosa* and *W. striatula* are lichens that inhabit the intertidal zone, remaining immersed during long periods. They are less exposed to direct sunlight than supralittoral species like *H. amphibia* or *H. maura* (Orange 2013; Higgins et al. 2014). Lichens and plants from shaded habitats generally have lower compensation points and display lower rates of photosynthesis under high irradiance than sun-adapted lichens and plants (Loach 1967; Green et al. 1997; Picotto & Tretiach 2010). Coste et al. (2016) found a relationship between the length of time that freshwater lichen species are submerged and the decay of photosynthesis activity under high irradiation. In their study, the subhydrophilic lichen *Verrucaria praetermissa* increased CO₂ assimilation notably when it was exposed to high PPF (2000 mmol m⁻² s⁻¹, aerial conditions), whereas it became negative in the hyperhydrophilous lichen *Verrucaria funckii* and in *Ionaspis lacustris* and *Porpidia hydrophila*, two mesohydrophilous species. Thus, the lowest photosynthetic rates – estimated by ETR and CO₂ assimilation – of Hm-Ws under high light is consistent with a less sunny microhabitat.

Non-photochemical quenching (NPQ) plays an important role in protecting vascular plants and lichens against excess radiation. NPQ mechanisms such as the xanthophyll cycle and state-transitions reduce the excitation pressure on reaction centers, thereby decreasing the possibility of photooxidative damage (Papageorgiou & Govindjee 2014).

Accordingly, NPQ is generally higher in sun-adapted than in shade-adapted plants and plant species (Demmig-Adams 1998; Picotto & Tretiach 2012). On the other hand, Hm-Ws displayed the most significant NPQ response to light in our comparison with Hm-Ha and Hm-Hm. The lower NPQ levels did not result in an increase in PSII excitation pressure as might be expected. Thus, it cannot be ruled out that energy dissipation in the photobionts of *H. amphibia* and *H. maura* lichens may be performed by alternative mechanisms different from NPQ.

Zonation of organisms' occurrence on rocky seashores has long attracted the attention of researchers (Knox 2000). Lichens, like other organisms, show distributions restricted to certain belts of the intertidal or supralittoral zones (Fletcher 1973a, b; Ryan 1989; Brodo & Sloan 2004). This distribution is influenced by desiccation tolerance, water temperature, salinity and pH (Fletcher 1976 1980). Recent studies have shown clear physiological differences between species growing in the supralittoral zone (*Hydropunctaria maura*) and middle intertidal zone (*Wahlenbergiella mucosa*) (Higgins et al. 2014). So far, lichen photobionts have received little attention in attempts to explain lichen zonation at the seashore (Thüs et al. 2011; Ortiz-Álvarez et al. 2015). Our results clearly indicate that lichen zonation may be driven by photobiont physiological features and mycobiont specialization (Ortiz-Álvarez et al. 2015).

Conclusions

Lichen-forming fungi occurring along the rocky seashore of the northern Iberian Peninsula have different strains of the recently described algal species *Halofilum ramosum*, which correspond to their positions with respect to the waterline. These algal strains differ in chloroplast ultrastructure and in their physiological responses to salt concentrations. Further research on the species boundaries in lichen photobionts, particularly those associated with aquatic lichens, will be needed to determine whether the ecophysiological differences found in this study correspond to different ecotypes or sibling species. Future studies should investigate the diversity of marine lichen photobionts in a wider range of species and regions to shed light on local and regional spatial variation, as well as on the degree to which photobiont selectivity has affected the evolutionary history of these lichens and their position at the seashore.

Acknowledgements

We dedicate this study to James Lawrey on the occasion of his 70th birthday, in recognition of all his work in the fields of lichenology and microbial ecology. We thank the MNCN Chromatographic Laboratory (Luis Cuadra and Elena Fernández) and M^a José Malo and Lydia Gonzalez for technical assistance, and Dr. William Sanders (Florida Gulf Coast University) for reviewing the English of the manuscript and for helpful comments on it. The microscopy and HPLC analyses were funded by the Spanish Education Ministry Grant CTM2012-38222-CO2-O2. SPO is supported by a 'Ramón y Cajal' contract (RYC-2014-16784) from the Spanish Ministry of Science, Innovation and Universities.

References

- Armstrong, R. A. & Smith, S. N. 1994. The levels of ribitol, arabitol and mannitol in individual lobes of the lichen *Parmelia conspersa* (Ehrh ex Ach) Ach. *Environmental and Experimental Botany* 34: 253–260.
- Batterton, J. & van Baalen, C. 1971. Growth Responses of Blue-Green Algae to Sodium Chloride Concentration. *Archives Microbiology* 76: 151–155.
- Ben-Amotz, A. & Avron, M. 1981. Glycerol and β -carotene metabolism in the halotolerant alga *Dunaliella*: a model system for biosolar energy conversion. *Trends in Biochemical Sciences* 6: 297–299.
- Ben-Amotz, A. & Grunwald, T. 1981. Osmoregulation in the halotolerant alga *Asteromonas gracilis*. *Plant Physiology* 67: 613–616.
- Bilger, W. & Bjorkman, O. 1990. Role of the xanthophyll cycle in photoprotection elucidated by measurements of light-induced absorbency changes, fluorescence and photosynthesis in leaves of *Hedera canariensis*. *Photosynthesis Research* 25: 173–185.
- Bisson, M. A. & Kirst, G. O. 1995. Osmotic acclimation and turgor pressure regulation in algae. *Naturwissenschaften* 82: 461–471.
- Bremauntz, M., Torres-Bustillos, L., Cañizares-Villanueva, R. & Fernández-Linares, L. 2011. Trehalose and sucrose osmolytes accumulated by algae as potential raw material for bioethanol. *Natural Resources* 2: 173–179.
- Brodo, I. M., & Santesson, R. 1997. Lichens of the Queen Charlotte Islands, British Columbia, Canada. 3. Marine species of *Verrucaria* (Verrucariaceae, Ascomycotina). *The Journal of the Hattori Botanical Laboratory* 82: 27–37.
- Brodo, I. M. & Sloan, N. A. 2004. Lichen zonation on coastal rocks in Gwaii Haanas National Park Reserve, Haida Gwaii (Queen Charlotte Islands), British Columbia. *The Canadian Field-Naturalist* 118: 405–424.
- Castresana, J. 2000. Selection of conserved blocks from multiple alignments for their use in phylogenetic analysis. *Molecular Biology and Evolution* 17: 540–552.
- Coste, C., Chauvet, E., Grieu, P. & Lamaze, T. 2016. Photosynthetic traits of freshwater lichens are consistent with the submersion conditions of their habitat. *Annales de Limnologie – International Journal of Limnology* 52: 235–242.
- Cowan, A. K., Rose, P. D. & Horne, L. G. 1992. *Dunaliella salina* – a model system for studying the response of plant-cells to stress. *Journal Experimental Botany* 43: 1535–1547.
- Darienko, T. & Pröschold, T. 2017. Toward a monograph of non-marine Ulvophyceae using an integrative approach (Molecular phylogeny and systematics of terrestrial Ulvophyceae II). *Phytotaxa* 324: 1–41.
- Darriba, D., Taboada, G. L., Doallo, R. & Posada, D. 2012. jModelTest 2: more models, new heuristics and parallel computing. *Nature Methods* 9: 772.
- de los Ríos, A. & Ascaso, C. 2002. Preparative techniques for transmission electron microscopy and confocal laser scanning microscopy of lichens. In: Kranner, I., Beckett, R. P. & Varma, A. K. (eds), *Protocols in Lichenology*, pp. 87–117. Springer-Verlag, Berlin, Heidelberg.
- del Campo, E. M., Casano, L. M., & Barreno, E. 2013. Evolutionary implications of intron–exon distribution and the properties and sequences of the RPL10A gene in eukaryotes. *Molecular Phylogenetics and Evolution* 66: 857–867.
- Delmail, D., Grube, M., Parrot, D., Cook-Moreau, J., Boustie, J., Labrousse, P., & Tomasi, S. Halotolerance in Lichens: Symbiotic Coalition Against Salt Stress. In: Prasad, M. N. V., Azooz, M. M. & Parvaiz Ahmad (eds), *Ecophysiology and Responses of Plants under Salt Stress*, pp. 115–148. Springer-Verlag New York.
- Demmig-Adams, B. 1990. Carotenoids and photoprotection in plants: a role for the xanthophyll zeaxanthin. *Biochimica et Biophysica Acta* 1020: 1–24.
- Demmig-Adams, B. 1998. Survey of thermal energy dissipation and pigment composition in sun and shade leaves. *Plant and Cell Physiology* 39: 474–482.
- Erdmann, N. & Hagemann, M. 2007. Salt acclimation of algae and cyanobacteria: a comparison. In: Rai, L. C. and Gaur, J. P. (eds) *Algal adaptation to environmental stresses: physiological, biochemical and molecular mechanisms*, pp. 322–360. Springer, Berlin.
- Fletcher, A. 1973a. The ecology of marine (littoral) lichens on some rocky shores of Anglesey. *The Lichenologist* 5: 368–400.
- Fletcher, A. 1973b. The ecology of maritime (supralittoral) lichens on some rocky shores of Anglesey. *The Lichenologist* 5: 401–422.
- Fletcher, A. 1980. Marine and maritime lichens of rocky shores: their ecology, physiology and biological interactions. In: Price, J. H., Irvine, D. E. G. & Farnham, W. F. (eds): *The Shore Environment. Volume 2: Ecosystems*, pp. 789–842. Academic Press, London & New York.
- Garrido-Benavent, I., Pérez-Ortega, S., & de los Ríos, A. 2017. From Alaska to Antarctica: species boundaries and genetic diversity of *Prasiola* (Trebouxiophyceae), a foliose chlorophyte associated with the bipolar lichen-forming fungus *Mastodia tessellata*. *Molecular Phylogenetics and Evolution* 107: 117–131.
- Genty B., Briantais J. M. & Baker N. R. 1989. The relationship between the quantum yield of photosynthetic electron-transport and quenching of Chlorophyll fluorescence. *Biochimica et Biophysica Acta* 990: 87–92.
- Goyal, A. 2007. Osmoregulation in *Dunaliella*, Part II: Photosynthesis and starch contribute carbon for glycerol synthesis during a salt stress in *Dunaliella tertiolecta*. *Plant Physiology and Biochemistry* 45: 705–710.
- Green, T. G. A., Büdel, B., Meyer, A., Zellner, H. & Lange, O. L. 1997. Temperate rainforest lichens in New Zealand: light response of photosynthesis. *New Zealand Journal of Botany* 35: 493–504.
- Green, T. G. A., Brabyn, L., Beard, C. & Sancho, L. G. 2012. Extremely low lichen growth rates in Taylor Valley, Dry Valleys, continental Antarctica. *Polar Biology* 35: 535–541.
- Gueidan, C., Roux, C. & Lutzoni, F. 2007. Using a multigene phylogenetic analysis to assess generic delineation and character evolution in Verrucariaceae (Verrucariales, Ascomycota). *Mycological Research* 111: 1145–1168.
- Gueidan, C., Savić, S., Thüs, H., Roux, C., Keller, C., Tibell, L., Prieto, M., Heiðmarsson, S., Breuss, O., Orange, A., Fröberg, L., Wynns, A. A., Navarro-Rosinés, P., Krzewicka, B., Pykälä, J., Grube, M. & Lutzoni, F. 2009. Generic classification of the Verrucariaceae (Ascomycota) based on molecular and morphological evidence: recent progress and remaining challenges. *Taxon* 58: 184–208.
- Hellebust J. A. 1985. Mechanisms of response to salinity in halotolerant microalgae. *Plant and Soil* 89: 69–81.
- Higgins, N. F., Connan, S., & Stengel, D. B. 2015. Factors influencing the distribution of coastal lichens *Hydropunctaria maura* and *Wahlenbergiella mucosa*. *Marine Ecology* 36: 1400–1414.
- Hill, D. J. & Ahmadjian, V. 1972. Relationship between carbohydrate movement and the symbiosis in lichens with green algae. *Planta* 103: 267–277.
- Hinton, R. H., Burge, M. L. E. & Hartman, G. C. 1969. Sucrose interference in the assay of enzymes and proteins. *Analytical Biochemistry* 29: 248–256.
- Joset, F., Jeanjean, R. & Hagemann, M. 1996. Dynamics of the response of cyanobacteria to salt-stress: Deciphering the molecular events. *Physiologia Plantarum* 96: 738–744.
- Kalyaanamoorthy, S., Minh, B. Q., Wong, T. K. F., von Haeseler, A. & Jermini, L. S. 2017. ModelFinder: fast model selection for accurate phylogenetic estimates. *Nature Methods* 14: 587–589.
- Katoh, K., Asimenos, G. & Toh, H. 2009. Multiple Alignment of DNA Sequences with MAFFT. In: Posada, D. (ed.). *Bioinformatics for DNA Sequence Analysis*, pp. 39–64. Totowa: Humana Press Inc.

- Kitajima, M. & Butler, W. L. 1975. Quenching of chlorophyll fluorescence and primary photochemistry in chloroplasts by dibromothymoquinone. *Biochimica et Biophysica Acta* 376: 105–115.
- Knox, G. A. (2000). *The ecology of seashores*. CRC press.
- Lamb, I. M. 1973. Further observations on *Verrucaria serpuloides* M. Lamb, the only known permanently submerged marine lichen. *Occasional papers of the Farlow Herbarium of Cryptogamic Botany* 6: 1–5.
- Loach, K. 1967. Shade tolerance in tree seedlings 1. Leaf photosynthesis and respiration in plants raised under artificial shade. *New Phytologist* 66: 607–621.
- Maphangwa, K. W., Musil, C. F., Raitt, L. & Zedda, L. 2012. Differential interception and evaporation of fog, dew and water vapour and elemental accumulation by lichens explain their relative abundance in a coastal desert. *Journal of Arid Environments* 82: 71–80.
- Meyer, M. T., Whittaker, C., Griffiths, H. 2017. The algal pyrenoid: key unanswered questions. *Journal of Experimental Botany* 68: 3739–3749.
- Minh, B. Q., Nguyen, M. A. T. & von Haeseler, A. 2013. Ultrafast Approximation for Phylogenetic Bootstrap. *Molecular Biology and Evolution* 30: 1188–1195.
- Moe, R. 1997. *Verrucaria tavaresiae* sp. nov., a marine lichen with a brown algal photobiont. *Bulletin of the California Lichen Society* 4: 7–11.
- Mohr, F., Ekman, S. & Heegaard, E. 2004.: Evolution and taxonomy of the marine *Collembosporium* species (lichenized Ascomycota) in north-west Europe. *Mycological Research* 108: 515–532.
- Nakayama, T., Watanabe, S., Mitsui, K., Uchida, H. & Inouye, I. 1996. The phylogenetic relationships between the Chlamydomonadales and Chlorococcales inferred from 18S rDNA sequence data. *Phycological Research* 44: 47–56.
- Nash, T. H. 2008. *Lichen Biology*. Cambridge University Press.
- Nguyen, L. T., Schmidt, H. A., von Haeseler, A., & Minh, B. Q. 2015. IQ-TREE: a fast and effective stochastic algorithm for estimating maximum-likelihood phylogenies. *Molecular biology and evolution* 32: 268–274.
- Orange, A. 2012: Semi-cryptic marine species of *Hydropunctaria* (Verrucariaceae, lichenized Ascomycota) from north-west Europe. *The Lichenologist* 44: 299–320.
- Orange, A. 2013. *British and other pyrenocarpous lichens. Version 2*. Available at <https://museum.wales/media/13849/Orange-A-2013-British-and-other-pyrenocarpous-lichens.pdf>
- Oren, A. 2008. Microbial life at high salt concentrations: phylogenetic and metabolic diversity. *Saline Systems* 4: 2
- Ortiz-Álvarez, R. de los Ríos, A. Fernández-Mendoza, F., Torralba-Burrial, A. & Pérez-Ortega, S. 2015: Ecological specialization of two photobiont-specific maritime cyanolichen species of the genus *Lichina*. *PLoS ONE* 10: e0132718.
- Page-Sharp, M., Behm, C. & Smith, G. 1999. Involvement of compatible solutes trehalose and sucrose in the response to salt stress of cyanobacterial *Scytonema* species isolated from desert soils. 1472: 519–528.
- Papageorgiou, G. C. & Govindjee. 2014. The non-photochemical quenching of the electronically excited state of chlorophyll a in plants: Definitions, timelines, viewpoints, open questions. In: Demmig-Adams, B., Garab, G., Adams III, W., Govindjee (eds), *Non-Photochemical Quenching and Energy Dissipation in Plants, Algae and Cyanobacteria*, pp. 1–44. Springer Netherlands, Dordrecht.
- Parra, O. O. & Redon J. 1977. Aislamiento de *Heterococcus caespitosus* Vischer ficobionte de *Verrucaria maura* Wahlenb. *Boletín de la Sociedad de Biología de Concepción* 51: 219–224.
- Pérez-Ortega, S., de los Ríos, A., Crespo, A. & Sancho, L. G. 2010. Symbiotic lifestyle and phylogenetic relationships of the bionts of *Mastodia tessellata* (Ascomycota, incertae sedis). *American Journal of Botany* 97: 738–752.
- Pérez-Ortega, S., Garrido-Benavent, I., Grube, M., Olmo, R. & de los Ríos, A. 2016. Hidden diversity of marine borderline lichens and a new order of fungi: Collemopsidiales (Dothideomyceta). *Fungal Diversity* 80: 285–300.
- Perez-Ortega, S., Miller, K. A. & de Los Rios, A. 2018. Challenging the lichen concept: *Turgidoscolum ulvae* (Verrucariaceae) represents an independent photobiont shift to a multicellular blade-like alga. *The Lichenologist* 50: 341–356.
- Pick, U. 2002. Adaptation of the halotolerant alga *Dunaliella* to high salinity. In: Läuchli, A., Lüttge, U. (eds), *Salinity: Environment – Plants – Molecules*. Springer, Dordrecht .
- Picotto, M. & Tretsch, M. 2010. Photosynthesis in chlorolichens: the influence of the habitat light regime. *Journal of Plant Research* 123: 763–775.
- Piercey-Normore, M. D. & Depriest, P. T. 2001. Algal switching among lichen symbioses. *American Journal of Botany* 88: 1490–1498.
- Ramazanov, Z., Rawat, M., Henk, M. C., Matthews, S. W. & Moroney, J. V. (1994) The induction of the CO₂-concentrating mechanism is correlated with the formation of the starch sheath around the pyrenoid of *Chlamydomonas reinhardtii*. *Planta* 195: 210–21.
- Reed, R. H., Richardson, D. L., Warr, S. R. & Stewart, W. D. 1984. Carbohydrate accumulation and osmotic stress in cyanobacteria. *Journal of General Microbiology* 130: 1–4.
- Reed, R. H. 1989. Osmotic adjustment and organic solute accumulation in *Chaetomorpha capillaris*. *British Phycological Journal* 24: 21–37.
- Renobales, G. & Noya, R. 1991. Estudio morfológico comparado de *Verrucaria maura* y *V. amphibia* en la Costa Vasca. *Acta Botánica Malacitana* 16: 149–156.
- Reynolds, E. S. 1963. The use of lead citrate at high pH as an electron-opaque stain in electron microscopy. *Journal of Cell Biology* 17: 208–212.
- Ronquist, F., Teslenko, M., van der Mark, P., Ayres, D. L., Darling, A., Höhna, S., Larget, B., Liu, L., Suchard, M. A. & Huelsenbeck, J. P. (2012) MrBayes 3.2: Efficient Bayesian phylogenetic inference and model choice across a large model space. *Systematic Biology* 61: 539–542.
- Roser, D. J., Melick, D. R., Ling, H. U. & Seppelt, R. D. 1992. Polyol and sugar content of terrestrial plants from continental Antarctica. *Antarctic Science* 4: 413–420.
- Ryan, B. D. 1988. Zonation of lichens on a rocky seashore on Fidalgo Island, Washington. *The Bryologist* 91: 167–180.
- Sanders, W. B., Moe, R. L. & Ascaso, C. 2004. The intertidal marine lichen formed by the pyrenomyces fungus *Verrucaria tavaresiae* (Ascomycotina) and the brown alga *Petroderma maculiforme* (Phaeophyceae): thallus organization and symbiont interaction. *American Journal of Botany* 91: 511–522.
- Santesson, R. 1939. Amphibious Pyrenolichens I. *Arkiv för Botanik* 29A: 1–67.
- Schreiber, U., Kühl, M., Klimant, I. & Reising, H. 1996. Measurement of chlorophyll fluorescence within leaves using a modified PAM fluorometer with a fiber-optic microprobe. *Photosynthesis Research* 47: 103–109.
- Schultz, M. 2017. Morphological and molecular data support *Lichina intermedia* as a distinct austral-marine species in the *L. pygmaea* group. *The Lichenologist* 49: 321–332.
- Stacey, G., Van Baalen, C. & Tabita, F. 1977. Isolation and characterization of a marine *Anabaena* sp. capable of rapid growth on molecular nitrogen. *Archives of Microbiology* 144: 197–201.
- Taylor, R. M. 1982. *Marine flora and fauna of the Northeastern United States. Lichens (Ascomycetes) of the intertidal region*. NOAA Technical Report NMFS Circular 446, U.S. Department of Commerce, Washington.

- Thüs, H. & Schultz, M. 2008. *Freshwater Flora of Central Europe, Vol. 21/1: Fungi, Part 1: Lichens*. Heidelberg: Spektrum.
- Thüs, H., Muggia, L., Pérez-Ortega, S., Favero-Longo, S. E., Joneson, S., O'Brien, H., Nelsen, M. P., Duque-Thüs, R., Grube, M., Friedl, T., Brodie, J., Andrew, C. J., Lücking, R., Lutzoni, F. & Gueidan, C. 2011. Revisiting photobiont diversity in the lichen family Verrucariaceae (Ascomycota). *European Journal of Phycology* 46: 399–415.
- Trifinopoulos, J., Nguyen, L. T., von Haeseler, A., & Minh, B. Q. 2016. W-IQ-TREE: a fast online phylogenetic tool for maximum likelihood analysis. *Nucleic Acids Research* 44: W232–W235.
- van Kooten, O. & Snel, J. F. H. 1990. The use of chloroFhy11 fluorescence nomenclature in plant stress physiology. *Photosynthesis Research* 25: 147–150.
- Warr, S. C. R., Reed, R. H. & Stewart, W. D. P. 1985. Carbohydrate accumulation in osmotically stressed cyanobacteria (Blue-Green Algae). *New Phytologist* 100: 285–292.
- White, T. J., Bruns, T. D., Lee, S. B. & Taylor, J. W. 1990. Amplification and direct sequencing of fungal ribosomal genes for phylogenies. In: Innis, M. A., Gelfand, D. H., Sninsky, J. J. & White, T. J. (eds), *PCR protocols: a guide to methods and applications*, pp. 315–322. Academic Press, San Diego.
- Zhan, Y., Marchand, C. H., Maes, A., Mauries, A., Sun, Y., Dhaliwal, J. S., Uniacke, J., Arragain, S., Jiang, H., Gold, N. D., Martin, V. J., Lemaire, S. D., Zerges, W. 2018. Pyrenoid functions revealed by proteomics in *Chlamydomonas reinhardtii*. *PLoS ONE* 13: e0185039.